CHAPTER V
HYBRID BIOMIMETIC ELECTROSPUN FIBROUS MATS DERIVED FROM POLY (ε-CAPROLACTONE) AND SILK FIBROIN PROTEIN FOR WOUND DRESSING APPLICATION

5.1 ABSTRACT

As the functionality of *Bombyx mori* silk fibroin (SF) on tissue scaffolding, in this study, we combined the unique properties of SF with poly (ε-caprolactone) (PCL) electrospun fibers, which demonstrate excellent biocompatibility and desirable physical properties, to develop biomimetic fibrous substrates for tissue engineering applications. The biomimetic fibrous structure was fabricated by conventional electrospinning of PCL. To achieve hybrid function of each individual electrospun fiber, the surfaces of PCL electrospun fibers were coated with silk fibroin protein using a lyophilization technique. The smooth surfaces of fibers were obtained with average fiber size increased from 508 ± 155 nm to 514 ± 132 nm after coating. The durability of SF coating films was investigated by further modification with fibronectin protein which can improve their biological-function. The rough surface of hybrid electrospun fibers was observed with an increasing of fiber diameters to 557 ± 129 nm after surface-modification. The hybrid electrospun fibers show improved support for normal human dermal fibroblast (NHDF) cells adhesion and proliferation than neat PCL, with the surface-modified hybrid electrospun fibers showing significantly enhanced proliferation of NHDF cells on their surface. This studied indicate the opportunity of using synthetic polymer as a platform for SF to construct a biomimetic fibrous structure which has the originality function as biomaterial.

5.2 Introduction

Recently, much attention has focused on the fabrication of scaffolds for biomedical applications such as tissue engineering and repair, with emphasis on the derivation of new biomaterial-based scaffolds. Silk fibroin (SF), naturally derived from *Bombyx mori* silkworms, is one of many candidate natural polymers for scaffold derivation due to its favorable biocompatibility, good oxygen and water vapor permeability and minimal inflammatory reaction in human tissue [1, 2]. Many researchers have explored ways to fabricate SF into scaffolds of various types which have been used in tissue engineering [1-5]. The major challenge in tailoring scaffolds for tissue engineering is in the fabrication process. One of the most effective methods for this is electrospinning, a proven technique that precisely creates the fibrous structure that can mimic nanofibrillar structure and the biological functions of the natural extracellular matrix. Electrospun fibrous mats also combine extremely large surface area to volume ratios with high porosity, features that are needed for the application of these materials in wound healing [6-10].

In selecting a biomaterial as a scaffold precursor for tissue engineering applications, excellent biocompatibility and cellular response are key prerequisite features [10, 11]. However, the biomaterial must be widely available, and also be able to be incorporated into the scaffold matrix. Biomaterials having a low yield of extraction are problematic, as this low availability complicates industrial scale production of the scaffold materials [12]. For example, using electrospinning, electrospun fibers of SF have to be fabricated with very high concentrations of SF (i.e. 20-40%) to obtain the properties desirable for tissue engineering [1, 3, 4]. Moreover, it was found that the mechanical properties of neat SF electrospun fibers were not ideal due to the highly crystalline β-sheet secondary structure in this material [13]. Recently, many methods have been developed to increase the viscoelasticity of the SF system by blending it with other polymers [14-16], which allows for the attainment of more desirable mechanical properties while retaining the biocompatibility derived from SF.

Currently, there are several wound dressings commercially available, made from blends of natural and synthetic polymers [11]. The most commonly used

synthetic polymer, which is biodegradable and biocompatible is poly (ε-caprolactone) (PCL). Due to its biocompatibility and outstanding mechanical properties, PCL is a good candidate for further fabrication into 3D fibrous scaffolds, with the fibrous structure being crucial for promoting cellular activity [9, 17, 18]. During the last few years, electrospinning of PCL has been successfully accomplished in various solvents, with the biocompatibility of the fibers having also been reported. However, PCL does not support cell growth due to its hydrophilicity and a lack of bioactive functionality. To address this issue, PCL has been chemically or physically immobilized by attaching natural proteins such as collagen onto the polymeric surface, which can then promote cell interactions and subsequently cell adhesion [19-23]. While these modifications stimulate cell attachment and proliferation, the materials developed still do not accurately mimic the biocompatibility of the natural polymer. Thus, the major challenge here is to replicate the natural functions on the surface of PCL, which is in direct contact with the cells or tissue.

Herein we present a new hybridization process to generate hybrid electrospun fibers from modified PCL and regenerated SF solution via lyophilization or freeze-drying. To combine the advantages of both components, PCL was used to fabricate the fibrous structure substrate, which was simple with excellent mechanical properties, while SF was employed as the outer layer to provide excellent biocompatibility and promote cellular responses [13, 24]. The effect of SF solution concentration on the morphology of the individual fibers, as well as the morphology, water retention and SF co-agglutination in the obtained fibrous matrices were examined in comparison to those of neat PCL. To further assess the durability and development of this hybrid electrospun fiber, fibronectin protein, which has been previously utilized as cellular binding sites for integrin receptors, was immobilized on the surface to improve cellular adhesion and proliferation [5, 14, 15, 25]. Then, the potential of the hybrid fiber to act as a wound healing material was evaluated *in vitro* through evaluating its cytotoxicity and the attachment and proliferation of normal human dermal fibroblast cells (NHDF), which are one of the most abundant cell types in connective tissue that can function to maintain tissue homeostasis when tissues are damaged [26]

5.3 Experimental

5.3.1 Materials

Poly (ε-caprolactone) was purchased from Acros Organics (Belgium). Fresh *Bombyx mori* silk cocoons (Chul 1/1) were kindly provided by Chul Thai Silk (Thailand). 1-Ethyl-3-(dimethylaminopropyl) carbodiimide hydrochloride (EDC), N-hydroxysuccinimide (NHS) and fibronectin were purchased from Sigma (Sigma, USA). The chemicals used for the preparation of SF and its spinning solutions, sodium carbonate (Na_2CO_3) and lithium bromide (LiBr), were purchased from Riedel-de Haën (Germany). Others chemicals used in the *in vitro* cell studies were purchased from Invitrogen Corp., (USA). All chemicals were of analytical grade and used without further purification.

5.3.2 Preparation of Stock Silk Fibroin Sponge

In brief, the silk cocoons were boiled for 30 min in an aqueous solution of 0.02 M Na_2CO_3, and then rinsed with warm distilled water followed by drying at 40 °C overnight. The degummed silk threads were dissolved by heating in 9.3 M aqueous LiBr solution at 55 °C for 30 min, affording an approximately 10% (w/v) silk fibroin solution. LiBr was then removed from the solution by dialysis in distilled water using a dialysis tubing cellulose membrane (Sigma-Aldrich, USA) for 3 days, followed by centrifugation at 5°C for 20 min. The SF solution was filtered and then lyophilized (freeze dried) to obtain the regenerated SF sponges. All sponges were stored in desiccators before use.

5.3.3 Preparation of PCL Electrospun Fibers via Electrospinning

In the electrospinning process, PCL electrospun fibers were prepared using a 12% (w/v) PCL solution in 50:50 (v/v) DCM/DMF. A blunt 20-gauge stainless steel hypodermic needle (o.d. 0.91 mm) was used as the nozzle. A high electric potential of 21 kV was applied to the needle. A jet of the PCL solution was then ejected onto an aluminum sheet attached to a rotating drum, which was used as a collector. The distance between the needle and the collector was fixed as 10 cm. The syringe and the needle were tilted at ~ 45° to maintain a constant flow rate of the electrospinning solution from the tip of the needle. The electrospun fibers were

processed continuously for 10 h under these ambient conditions. The obtained PCL electrospun fibers were found to be around 140 μm in thickness.

5.3.4 Hybridization of Fibers and Surface Modification

The PCL electrospun fibers were immersed in a silk solution prepared by dissolve SF sponge in DI water at concentrations of 0.5 %, 0.75 % and 1 % (w/v). The formed mats were then frozen at -40°C for 24 h, and then lyophilized to obtain the hybrid electrospun fiber mats. These were further immersed in 98% methanol for 10 min to induce a conformational change in the SF from amorphous (unstable silk I) to β-sheet (silk II), which is water-insoluble [1]. Immobilization of the biomolecule (i.e. fibronectin) onto the surface of the hybrid fibers was carried out by first immersing the hybrid fiber mats into a PBS buffer for 30 min to hydrate and stimulate the -COOH groups in the aspartic acid and glutamic acid residues on the SF surface. Following this, the functional groups on the fiber surface were activated by treating the hybrid fiber mats with 1-ethyl-3-(dimethylaminopropyl) carbodiimide hydrochloride (EDC)/ N-hydroxysuccinimide (NHS) solution (0.5 mg/mL of EDC with 0.7 mg/mL of NHS in PBS buffer) for 15 min at ambient temperature. The activated electrospun fiber mats were rinsed with PBS buffer, treated with 0.1 mg/ml fibronectin in PBS buffer for 2 h at ambient temperature and then rinsed with PBS buffer three times, followed by distilled water to remove excess peptides and salts before being air-dried [27].

5.3.5 Scanning Electron Microscopy

A Hitachi S-4800 Ultra-high resolution cold field Scanning Electron Microscope (FE-SEM) was used to investigate the morphology and size of individual fibers at each stage of the fabrication process. The samples were fixed onto the stub and sputter coated with platinum before analysis. The fiber sizes were statistically analyzed by using the SemAphore 4.0 program. All measurements were randomly made from at least 100 readings of individual fiber diameters.

5.3.6 Fourier Transform Infrared Spectroscopy (FTIR)

All infrared spectra were acquired using a Thermo Nicolet Nexus 670 Spectrophotometer. All spectra were recorded in the attenuated total reflectance Fourier Transform (ATR-FTIR) mode using a ZnSe crystal cell. Each measurement was achieved by accumulation of 32 scans, with a resolution of 4 cm^{-1} and a spectral

range of 400 to 4,000 cm^{-1}. The hybrid electrospun fibers were analyzed over all stages of fabrication, with the neat PCL electrospun fibers employed as a control.

5.3.7 Water-uptake Capacity and Dissolution Behavior

Hybrid and neat PCL electrospun fibers in their dried state were cut into 15 mm circular discs and weighed to record the initial dry weight (W_i) of each specimen. Subsequently, these fibers were immersed in PBS buffer at 37°C for various time intervals. At each allotted time interval, the wet weight of the fiber mats in the swollen state (W_s) was determined after the elimination of excess water through blotting the fibers with tissue paper. After the submersion, each specimen was dried to constant weight at 50°C for 24 h to obtain the final dry weight (W_d). The water retention capacities (%) for the electrospun fibers were calculated using the following equations:

$$\text{Water content (\%)} = (W_s\text{-}W_i)/W_i \times 100$$

and

$$\text{Mass remaining (\%)} = 100\text{-}(W_i\text{-}W_d/W_i \times 100)$$

5.3.8 X-ray Photoelectron Spectroscopy (XPS)

To determine the chemical grafting efficiency, the XPS spectra of hybrid and neat PCL electrospun fibers were recorded using a Thermo Fisher Scientific Thetaprobe XPS (Singapore) equipped with a monochromatic Al Kα X-ray source. The photoemitted core level electrons were collected at a fixed take-off angle of 50° with respect to the surface plane. The investigation area was approximately 400 μm x 400 μm with ~4-8 nm maximum analysis depth. A specially designed electron flood gun with a few eV Ar$^+$ ion was used for charge compensation. Further corrections were made based on adventitious C 1s at 285.0 eV using standard manufacturer software. Survey spectra were acquired for surface composition analysis with Scofield sensitivity factors.

5.3.9 Indirect Cytotoxicity Evaluation

The *in vitro* compatibility of the fiber mats was investigated according to the procedure outlined in standard test method (ISO 10993-5). The cytotoxicity of each specimen was evaluated by an indirect method, adapted from the standard test

method, by using normal human dermal fibroblast cells (NHDF, 15th passage). The cells were maintained in Dulbecco's modified Eagle's medium (DMEM) by adding prerequisite amounts of 10% fetal bovine serum (FBS), 1% l-glutamine, and 1% antibiotic and antimycotic formulation (penicillin G sodium, streptomycin sulfate, and amphotericin B) at 37°C in a humidified atmosphere containing 5% CO_2. Prior to extraction, the specimens were sterilized using UV radiation for 2 h. Then, they were immersed in a serum-free medium (SFM; DMEM containing 1% l-glutamine, 1% lactalbumin and 1% antibiotic and antimycotic formulation) for 24 h at extraction ratios of 5, 10 and 20 mg/ml, and then the extraction medium was used for the cell culture study. Normal human dermal fibroblasts were cultured separately in 24-well tissue-culture polystyrene plates (TCPS) at a density of 10,000 cells/well in DMEM for 24 h. After this, the culture medium was replaced with each extraction medium, and the cells re-incubated for 24 h. Finally, the cell viability in each well was assessed using the 3-(4,5-dimethylthiazol-2-yl)-2,5-diphenyltetrazolium bromide (MTT) assay.

5.3.10 Cell Attachment and Proliferation Study

For the cell attachment study, fiber mats (control, PCL, hybrid, surface-modified hybrid) were cut into circular discs (~15 mm in diameter) which then sterilized through UV irradiation of each side for 1 h. The specimens were then placed in individual wells of 24-well TCPS. To ensure a complete contact between each specimen and the bottom of each well, a metal ring (~12 mm in diameter) was placed on top of each specimen. The normal human dermal fibroblast cells were then cultured on the surface of each of the electrospun fibers, and glass slides (i.e., positive control) for 2, 4 and 8 h in the same medium as stated previously (incubation in 5% CO_2 at 37 °C). Each specimen after cell seeding was rinsed with phosphate buffered saline solution (PBS) to removed unattached cells prior to quantification of cell viability using the MTT assay. For the cell proliferation study, the cells were first allowed to attach to the substrates for 24 h. The number of proliferated cells was then determined by MTT assay on days 1, 2, and 3 after cell culturing.

5.3.11 Morphological Observation of Cultured Cells

After the culture medium had been removed, the cell-cultured electrospun fibers were rinsed twice with PBS and the cells were then fixed with 3%

glutaraldehyde/PBS solution (Electron Microscopy Science, USA) for 30 min. After fixing, the cell-cultured specimens were rinsed again with PBS prior to being dehydrated in aqueous ethanol solution of various concentrations (i.e., 30, 50, 70 and 90 %v/v respectively) and in pure ethanol for 2 min each. The specimens were then dried in 100% hexamethyldisilazane (HMDS; Sigma-Aldrich, USA) for 5 min and later dried in air allowing removal of HMDS. After being completely dried, the specimens were fixed on stubs and sputter coated with platinum before observation using FE-SEM. For comparison, cells that had been seeded or cultured on a glass substrate (cover glass slide, 1 mm in diameter; Menzel, Germany) were used as positive control.

5.3.12 Statistics and Data Analysis

All of the quantitative data were expressed as means±standard deviations (SD). Statistical comparisons were carried out by the one-way analysis of variance (one-way ANOVA) using SPSS 13.0 for Windows software (SPSS, USA). The statistical difference between two sets of data was considered when $p < 0.05$.

5.4 Results and Discussions

5.4.1 Physiochemical Properties of Electrospun Fibers

PCL electrospun fibers were successfully fabricated as shown in Figure 5.1a with uniform morphology and bead free, with fiber diameters being approximately 508±155 nm (Table 1). After the hybridization process, the effect of SF concentration on the fiber coating and morphology were investigated. With increasing concentrations of SF, the cumulative amount of SF on the fiber surface was shown to increase (Figure 5.2) but plateau after 0.5% (w/v). In general, the lyophilization technique is used to produce a porous structure of SF. However in this study, SF protein was successfully coated on the neat PCL fiber surface at low concentrations of SF, while SF film formation on the PCL surface occurred at higher concentration (1.0% w/v) of SF (Figure 5.2). Accordingly, an SF protein concentration of 0.5% w/v in aqueous solution was chosen for further fabrication. To enhance the clinical potency of hybrid electrospun fibers, fibronectin protein was grafted on the SF surface via a coupling reaction. The fiber morphologies of hybrid

electrospun fibers showed significant changes, having increased roughness with respect to PCL fibers (Figure 5.1c). The size of these fibers after coating with silk fibroin showed a slight increase from 514±132 nm to 557±129 nm after surface-modification, as summarized in Table 1.

The chemical integrity of the electrospun fibers in each state was investigated using ATR-FTIR spectroscopy (Figure 5.3). The peak of amide I and amide II, centered at around 1643 cm^{-1} and 1536 cm^{-1} respectively, wereobserved after hybridization by SF protein. Upon MeOH treatment of the hybrid electrospun fibers, the amide I and amide II absorption peaks shifted to 1627 cm^{-1} and 1521 cm^{-1}, respectively, which was indicative of the changes in secondary structure of the SF protein from the α-helix to β-sheet conformation [1, 14]. For the surface-modified hybrid electrospun fibers, a peak resulting from N–H stretching of the NH$_2$ groups, centered around 3287 cm^{-1}, was observed. The amplification of peak intensity indicated an increase in the number of NH$_2$ groups on the surface, as expected from the grafting of fibronectin [19].

5.4.2 Surface Elemental Composition

Figure 5.4 shows the XPS spectra of the electrospun fibers in each fabrication state. The neat PCL electrospun fibers show typical peaks of C 1s and O 1s at binding energies of 284.6±0.2 eV and 531.0±0.2 eV, whereas the hybrid and surface-modified electrospun fibers show evidence of N 1s at a binding energy of 398.3±0.2 eV, due to the presence of SF and fibronectin proteins on the surface [27]. In addition, the results of elemental concentrations (at. %), N/C and O/C ratios, and chemical functions (at. %) on the surface before, and after, modification are reported in Table 2. The elemental compositions of carbon (C), nitrogen (N) and oxygen (O) (in at. %) related to the hybrid electrospun fiber surface are 62.6 %, 15.5 % and 21.9 %, in comparison with the surface-modified hybrid electrospun fiber surface whose compositions are 62.2 %, 16.3 %, and 21.5 %, respectively. The increase in N/C ratio seen in the surface-modified electrospun fibers was expected, being a result of the grafting of fibronectin on the surface. Additionally, the coupling reaction was investigated through examination of the XPS curves, in particular the peaks related to carbon (C 1s) for the electrospun fibers. Three components of the C 1s peak corresponding to C–(C,H) centered at 285.0±0.2 eV, C–(O,N) centered at 286.5±0.2

eV, and O–$\underline{C}$=O centered at 288.1±0.2 eV found in hybrid and surface-modified hybrid electrospun fiber surfaces are shown in Figure 5.5. The percentage of $\underline{C}$–(O,N), assigned to the carboxylate functions of the protein, increased after hybridization of SF and was then seen to decrease after surface modification due to the coupling reaction on the surface, while the percentages of O–$\underline{C}$=O and $\underline{C}$–(C,H) increased significantly, that may related to the presence of the fibronectin side chains on the surface [28]. The data obtained from O 1s and N 1s peaks were in agreement with the results from the C 1s peak.

5.4.3 Water Retention Capacity and Dissolution Behavior

To determine the performance of a wound dressing material suited especially for exudate wounds, the water retention capacity and dissolution behavior of the electrospun fibers was investigated in PBS buffer solution at 37 °C (physiological temperature) over a 3 day period. Figure 5.6 shows the difference in water retention capacity for each substrate. After the initial time period (15 min) the neat PCL electrospun fibers showed a pronounced increase in water content (28%), with saturation (35%) occurring after 2 h of submersion. Interestingly, the hybrid electrospun fibers having strongly hydrophilic SF protein exhibited greater water capacity, with the water uptake rate increasing much more rapidly after immersion over the first time period (15 min, 151%), followed by a slower rate of increase. The water capacity value for the surface-modified fibers was slightly lower than hybrid electrospun fibers, i.e., 123.21% after 2 h, but the water retention capacity was found to further increase and finally became saturated at the same level as for the hybrid electrospun fibers after 24 h of submersion (184% and 186%, respectively). Simultaneously to the above experiment, the dissolution of each substrate was observed during the submersion time (Figure 5.7). According to these results, submersion in PBS buffer solution results in only a minor decrease in the weight of the PCL electrospun fibers. However, the hybrid electrospun fiber mat showed slight dissolution after 15 min due to partial disintegration of the SF protein. More rapid weight loss occurred on further immersion, indicating partial disintegration attributed to desorption of fibronectin proteins. After 48 h of submersion time, the weights of PCL, hybrid and surface-modified hybrid electrospun fibers had decreased to 98.50 %, 97.08 % and 97.45 % of the initial levels, respectively. However, in the context of

their applications as wound dressing materials these results would suggest that surface modification has no significant effect on the dissolution behavior of the hybrid electrospun fibers.

5.4.4 Indirect Cytotoxicity Evaluation

To test the biocompatibility of the fibers, NHDF cells were used as reference in the assessment cultured in extraction medium, in comparison with fresh culture medium as a control. The cell viabilities in the presence of all types of fibrous substrates at different extraction ratios (i.e., 5, 10, 20 mg/ml) are shown in Figure 5.8. For all substrates, the viability of NHDF cells was in the range of 88 % to 115 %, in comparison with the viability of cells that had been cultured with the control, and cell viability decreased with increasing extraction ratio. Comparatively, the viabilities of NHDF cells exposed to neat PCL and hybrid electrospun fibers were nearly equivalent and within the range 88-96 %, indicating that the substrates were non-toxic to the cells. However, the cell viability of the surface-modified hybrid electrospun fibers was the highest in all extraction ratios including the control. It should be noted that some of the growth substance (fibronectin) was desorbed during extraction, and in regards to the cell viability, this is important for promoting cell proliferation.

5.4.5 Cell Attachment and Cell Proliferation

As fibers were shown to be non-toxic to NHDF cells, a quantitative analysis of the adherence of NHDF seeded onto the surface of each type of fibrous substrate was undertaken. The results of cell viability on each substrate and the control after time intervals of 2, 4 and 6 h are shown in Figure 5.9. For any given substrate, the absorbance value, which is proportional to the number of cells, intensified over time. After 2 h the cell viabilities in the presence of all fibrous substrates were far higher than in the control due to the substrate's mimicry of extra cellular matrix (ECM) which supports cell growth. For hybrid electrospun fibers, the viability of cells on the surface was not significantly greater than for neat PCL fibers, however surface-modified hybrid electrospun fibers exhibited significantly higher viability. After 4 h, the cell viability on hybrid electrospun fibers was closer to that of surface-modified hybrid electrospun fibers than neat PCL fibers, but they were both significantly higher than cells seeded on neat PCL fibers. At 6 h, only the cell

viability on surface-modified fibers was significantly higher than for other fibers. However, regardless of the culturing time fibrous substrates appeared to support the attachment of the NHDF cells better than the control, especially in the case of surface-modified fibers.

Figure 5.10 highlights results of the quantitative analysis for the proliferation of fibrous substrate cultured NHDF over time. Evidently, for surface-modified hybrid electrospun fibers, the viability of cells on the surface was significantly greater over all time points than for other types of fibrous substrate and the control. On day 1, the cell viability on all substrates was greater than that of the control, with the viability on surface-modified fibers being markedly higher. On day 2, the cell viability on neat PCL, and hybrid electrospun fibers showed equivalence with that of the control, however on day 3 the cell viability of surface-modified hybrid electrospun fibers was much greater than those of other fibrous substrates, but close to that of the control. On the basis of this study, fiber size and the orientation of fibrous substrates can play a role in dictating cellular behavior [17, 29], however SF protein provides an improvement to the hydrophilicity and biocompatibility of the substrate, assisting fibroblast adhesion and proliferation. Additionally, the surface-modified hybrid electrospun fibers were clearly superior to other fibrous substrates investigated for supporting the growth of NHDF cells. Fibronectin may act as a cellular mediator, playing an important role on the proliferation of the NHDF cells on the substrate surface [25]. The penetration of cells inside the porous matrix may be also induced by fibronectin protein, which contains the cell binding domain RGD

5.4.6 Morphology of Cultured Cells

Selected SEM images showing the attachment and proliferation activity of NHDF cultured on the surface of fibrous substrates at various culture times are shown in Tables 3 and 4 respectively. According to Table 3, NHDF cells seeded on PCL electrospun fibers after 2 h had a round shape. After the same culture time, the cells on the surface of hybrid electrospun fibers showed slight expansion of their cytoplasm, and these became fully expanded in cells on the surface of surface-modified hybrid electrospun fibers. After 4h, the cells on the surface of hybrid and surface-modified electrospun fibers showed strong evidence of lemellipodia, in contrast to those cultured on PCL electrospun fibers. After 8h, the cells attached to

hybrid electrospun fibers further extended their cytoplasm along the fiber surfaces while those on surface-modified hybrid electrospun fibers were in the shape of migrating cells. From these results, the hybrid electrospun and surface modified fibers appeared to support the attachment of NHDF cells better than neat PCL electrospun fibers. During proliferation (Table 4), for any given type of substrate, the number of cells was seen to increase with culture time. Evidently, cells seeded on hybrid electrospun fibers show well expanded cytoplasms, resulting in the adoption of thin, long spindle-like shapes at day 1, most notably on surface-modified hybrid electrospun fibers. On days 2 and 3, for surface-modified hybrid electrospun fibers, the long spindle-like cytoplasms of the cells were mainly observed along the surface of the fibers. Nevertheless, on day 3, the cells appeared to nicely cover and migrate on the surface of that substrate, while cellular growth on PCL and hybrid electrospun fibers showed some agglomeration, or clogging, on the surface of substrates. As previously mentioned, the improved wettability and biocompatibility of the surface-modified hybrid electrospun fibers act to promote proliferation and migration of the cells over the surface. This is essential for medical applications, where the formation of a new three-dimensional connective tissue network is required for effective wound healing and tissue regeneration.

5.5 Conclusions

Hybrid electrospun fibers having the potential to be used as new bioactive wound healing materials have been fabricated. Silk fibroin protein (0.5% w/v) was effectively coated onto PCL electrospun fibers surface via a lyophilization process. The average diameters of individual fibers increased from 508±155 nm to 514±132 nm after coating. Fibronectin was successfully immobilized onto the surface of the hybrid electrospun fibers, with the existence of the immobilized fibronectin being confirmed by ATR-FTIR spectroscopy and XPS measurements. The grafting of fibronectin resulted in a three-fold higher water retention capacity of the surface-modified fibers over neat fibers, creating a material having the ability to absorb exudates which is a necessary feature in wound dressings. Because of their biocompatible surface, hybrid electrospun fibers exhibited superior support

properties for cellular attachment and proliferation than neat PCL fibers, with this being further improved through the grafting of fibronectin to form surface-modified hybrid electrospun fibers. Moreover, surface-modified hybrid electrospun fibers allowed for the best migration of NHDF cells over the fibers surface, which is crucial for the building up of new tissue in wound repair. These findings open an exciting opportunity to fabricate biocompatible scaffold structures that could be used as next generation effective wound healing materials.

5.6 Acknowledgements

5.7 References

1. Vepari, C.; Kaplan, D.L. *Prog. Polym. Sci.* **2007**, *32*, 991-1007

2. Hardy, J.G.; Scheibel, T.R. *Prog. Polym. Sci.* **2010**, *35*, 1093-1115

3. Okhawilai, M.; Rangkupan, R.; Kanokpanont, S.; Damrongsakkul, S. *Int. J. Biol. Macromol.* **2010**, *46*, 544-550

4. Zhu, J.; Shao, H.; Hu, X. *Int. J. Biol. Macromol.* **2007**, *41*, 469-474

5. Schneider, A.; Wang, X.Y.; Kaplan, D.L.; Garlick, J.A.; Egles, C. *Acta Biomater.* **2009**, *5*, 2570-2578

6. Bar-Cohen, Y. *Bioinsp. Biomim.* **2006**, *1*, P1-P12

7. Liu, K.; Jiang, L. *Nano Today* **2011**, *6*, 155-175

8. Liao, S.; Chan, C.K.; Ramakrishna, S. *Mater. Sci. Eng., C* **2008**, *28*, 1189-1202

9. Agarwal, S.; Wendorff, J.H.; Greiner, A. *Polymer* **2008**, *49*, 5603-5621

10. Zahedi, P.; Rezaeian, I.; Ranaei-Siadat, S-O.; Jafari, S-H.; Supaphol, P. *Polym. Adv. Technol.* **2009**, *21*, 77-95

11. Ovington, L.G. *Clin. Dermatol.* **2007**, *25*, 33-38

12. Khadka, D.B.; Haynie, D.T. *Nanomedicine* **2012**, *8*, 1242-1262

13. Meinel, A.J.; Kubowb, K.E.; Klotzsch, E.; Garcia-Fuentes, M.; Smith, M.L.; Vogel, V.; Merkle, H.P.; Meinel, L. *Biomaterials* **2009**, *30*, 3058-3067

14. Li, C.; Vepari, C.; Jin, H-J.; Kim, H.J; Kaplan, D.L. *Biomaterials* **2006**, *27*, 3115-3124

15. Jin, H. *Biomaterials* **2004**, *25*, 1039-1047

16. Aznar-Cervantes, S.D.; Vicente-Cervantes, D.; Meseguer-Olmo, L.; Cenis, J.L.; Lozano-Pérez, A.A. *Mater. Sci. Eng., C* **2013**, *33*, 1945-1950

17. K-hasuwan, P-r.; Pavasant, P.; Supaphol, P. *Langmuir* **2011**, *27*, 10938-10946

18. Wutticharoenmongkol, P.; Sanchavanakit, N.; Pavasant, P.; Supaphol, P. *J. Nanosci. Nanotechnol.* **2006**, *6*, 514-522

19. Mattanavee, W.; Suwantong, O.; Puthong, S.; Bunaprasert, T.; Hoven, V.P.; Supaphol, P.; *ACS Appl. Mater. Interfaces* **2009**, *1*, 1076-1085

20. Andukuri, A.; Kushwaha, M.; Tambralli, A.; Anderson, J.M.; Dean, D.R.; Berry, J.L.; Sohn, Y.D.; Yoon, Y-S, Brott, B.C.; Jun, H-W. *Acta Biomater.* **2011**, *7*, 225-233

21. Chuenjitkuntaworn, B.; Inrung, W.; Damrongsri, D.; Mekaapiruk, K.; Supaphol, P., Pavasant, P. *J. biomed. mater. res., Part A* **2010**, *94A*, 241-251

22. Kim, M.; Kim, G. *Carbohydr. Polym.* **2012**, *90*, 592-601

23. Li, L.; Li, H.; Qian, Y.; Li, X.; Singh, G.K.; Zhong, L.; Liu, W.; Lv, Y.; Cai, K.; Yang, L. *Int. J. Biol. Macromol.* **2011**, *49*, 223-232

24. Croisier, F.; A.-S. Duwez, Jérôme, C.; Léonard, A.F.; van der Werf, K.O.; Dijkstra, P.J.; Bennink, M.L. *Acta Biomater.* **2012**, *8*, 218-224

25. Satriano, C.; Messina, G. M.L.; Marino, C.; Aiello, I.; Conte, E.; Mendola, D.L.; Distefano, D.A.; D'Alessandro, F.; Pappalardo, G.; Impellizzeri, G. *J. Colloid Interface Sci.* **2010**, *341*, 232-239

26. Li, B.; Wang, J.H.C. *J. Tissue Viability* **2011**, *20*, 108-120

27. Bai. L.; Zhu, L.; Min, S.; Liu, L.; Cai, Y.; Yao, J. *Appl. Surf. Sci.* **2008**, *254*, 2988-2995

28. Ahimou, F.; Boonaert, C. J.P.; Adriaensen, Y.; Jacques, P.; Thonart, P.; Paquot, M.; Rouxhet, P.G. *J. Colloid Interface Sci.* **2007**, *309*, 49-55

29. Lowery, J.L.; Datta, N.; Rutledge, G.C. *Biomaterials* **2010**, *31*, 491-504

(a)

(b)

(c)
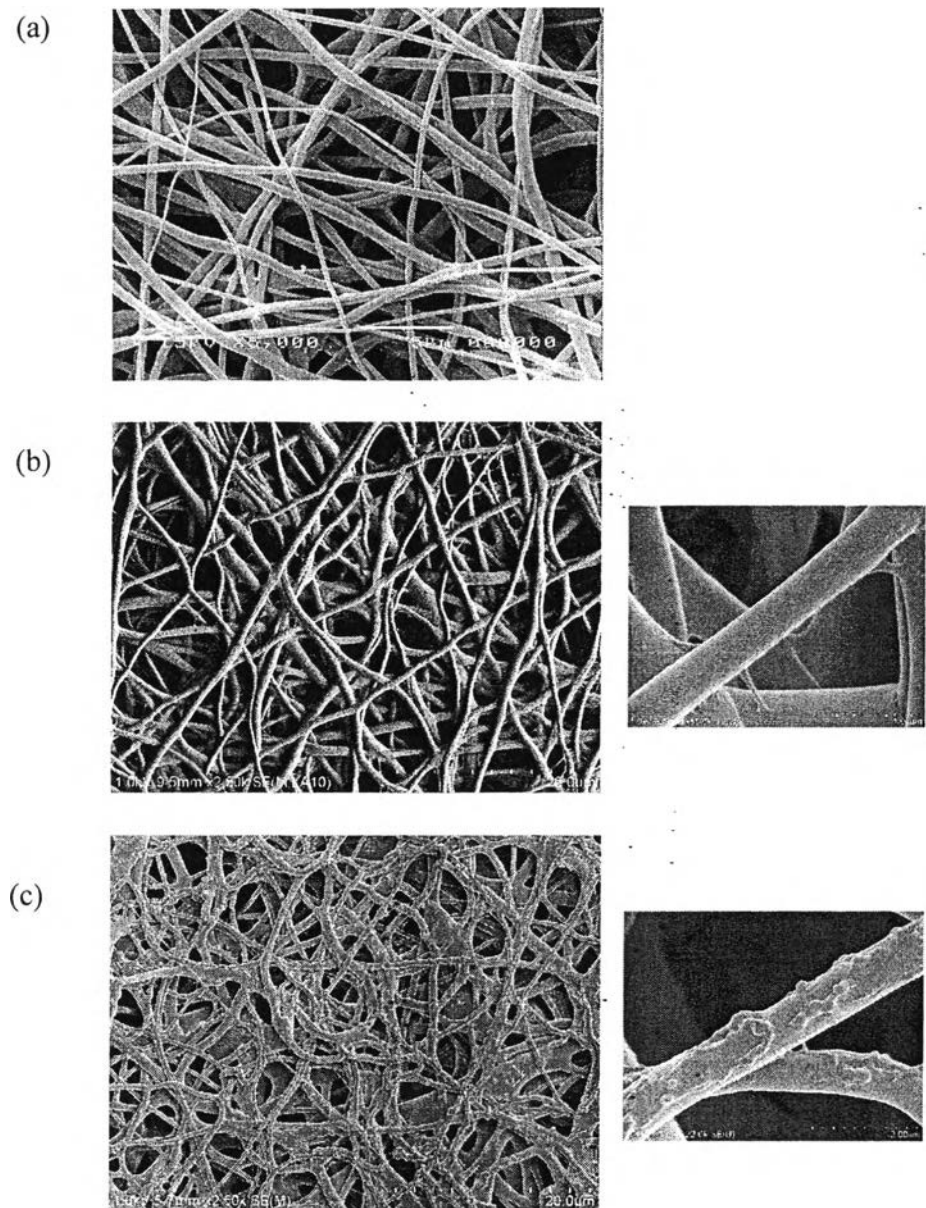
Figure 5.1 SEM micrographs of (a) neat PCL electrospun fibers, (b) hybrid electrospun fibers and (c) surface-modified hybrid electrospun fibers at 5000x, 2500x and 22000x of magnification. The applied EFS were 21 kV/20 cm.

Table 5.1 Electrospun Fiber diameters

Electrospun Fiber type	Average fiber diameter (nm)	Minimum fiber diameter (nm)	Maximum fiber diameter (nm)
Neat PCL	508±155	100	890
Hybrid	514±132	280	830
Surface modified hybrid	557±129	320	1040
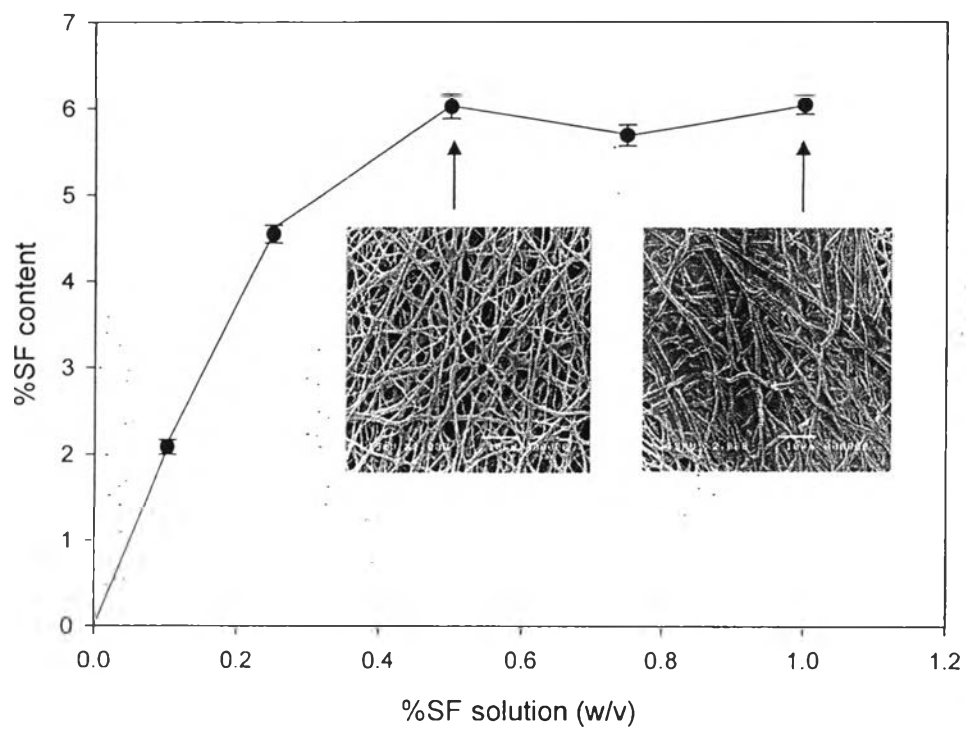
Figure 5.2 The % SF content on the surface of hybrid electrospun fibers as a function of SF solution concentration.
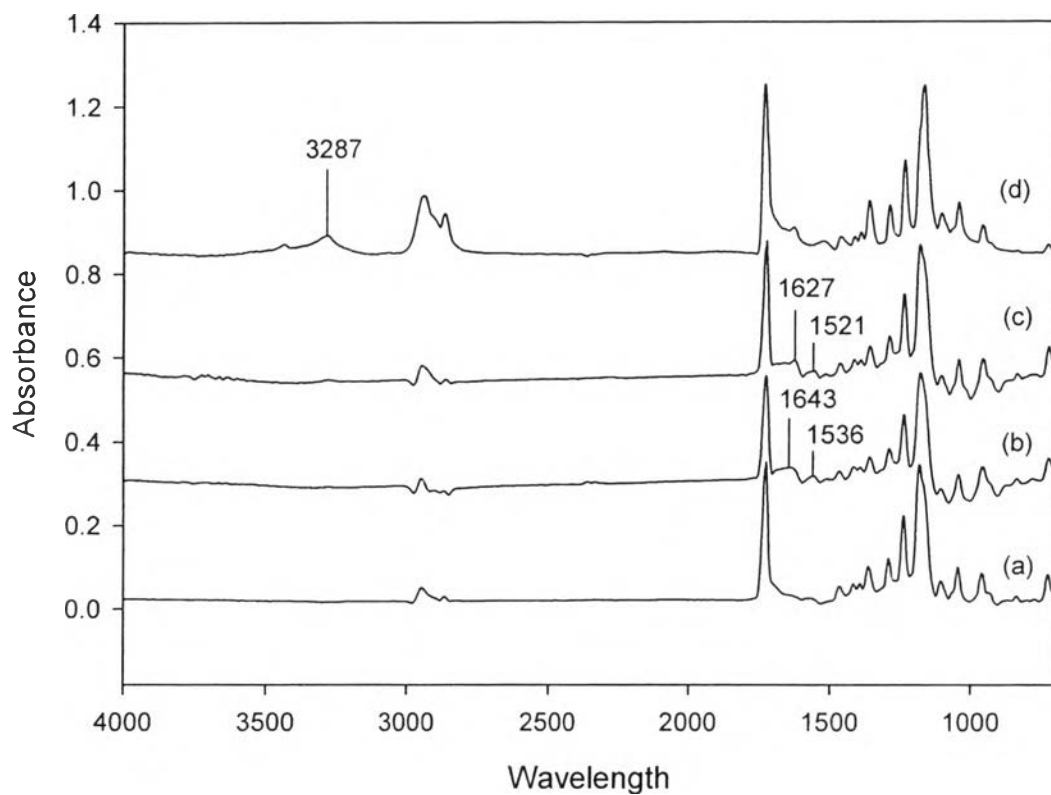
Figure 5.3 FTIR spectra for different electrospun fiber mats made from: (a) neat PCL electrospun fibers, (b) hybrid electrospun fibers, (c) MeOH treated hybrid electrospun fibers and (d) surface-modified hybrid electrospun fibers.
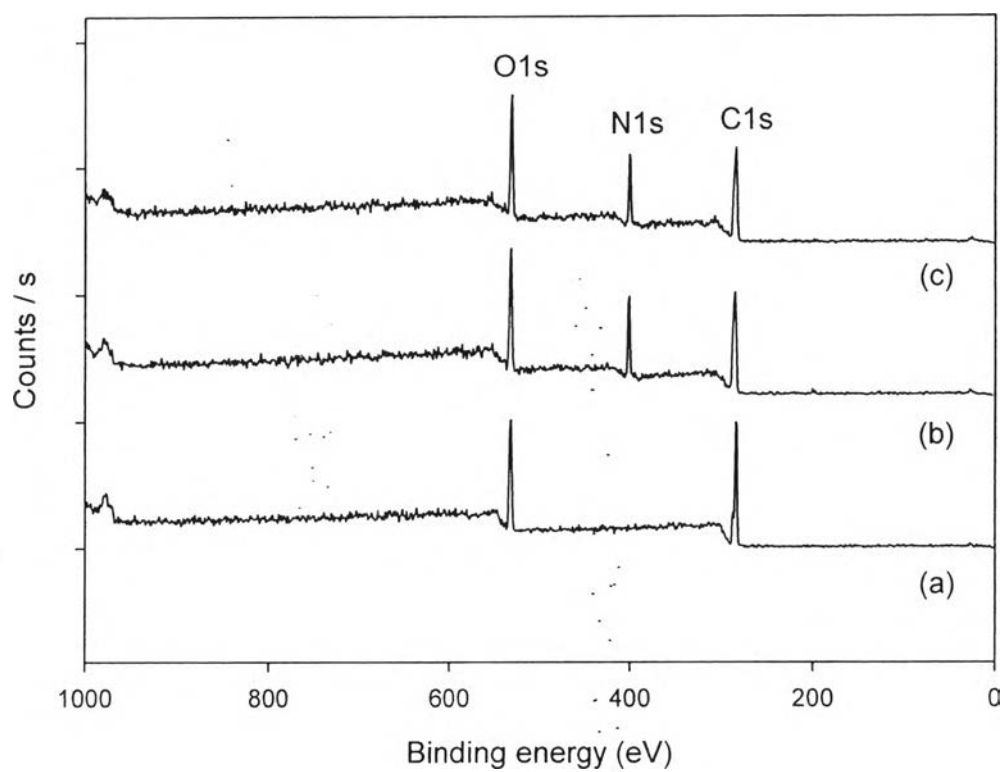
Figure 5.4 XPS spectra of (a) neat PCL electrospun fibers, (b) hybrid electrospun fibers and (c) surface-modified hybrid electrospun fibers.

Table 5.2 XPS surface chemical compositions and elemental ratios for each type of electrospun fiber before, and after modified with fibronectin

Sample	Surface atomic composition (at.%)			Elemental composition ratio		Chemical functions (at.%)				
	C 1s	N 1s	O 1s	N/C	O/C	285.0[a] C–(C,H)	286.5[a] C–(O,N)	288.1[a] O–C=O	533.1[a] C–O	531.9[a] C=O
PCL nanofibers	76.6	0	23.4	0	0.31	47.8	15.0	12.3	11.8	12.2
Hybrid nanofibers	62.6	15.5	21.9	0.25	0.35	21.6	23.9	17.3	4.0	17.0
Surface-modified hybrid nanofibers	62.2	16.3	21.5	0.26	0.35	26.0	20.7	16.0	3.6	17.5

[a] Binding energy (electron volts)
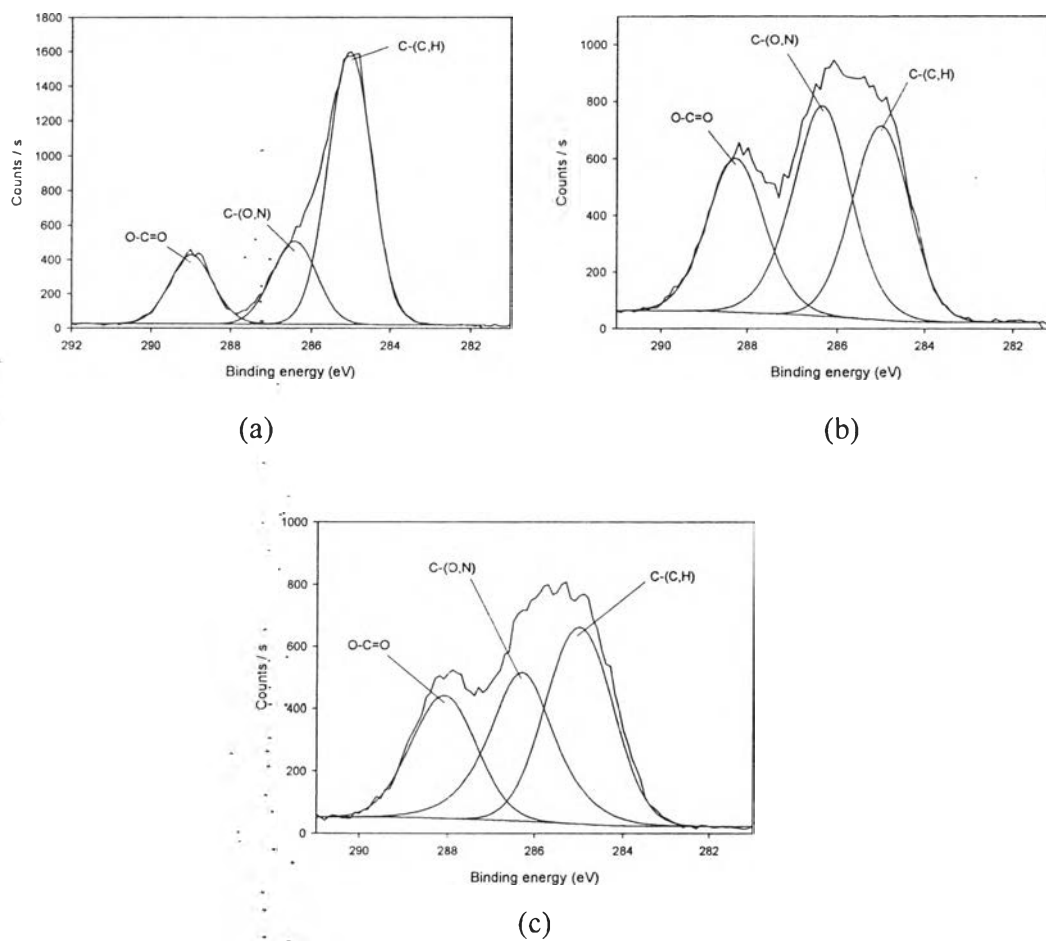
Figure 5.5 XPS photoelectron peak fitting of C 1s of (a) neat PCL electrospun fibers, (b) hybrid electrospun fibers and (c) surface-modified hybrid electrospun fibers. The different chemical compositions obtained from the peak fitting are shown.
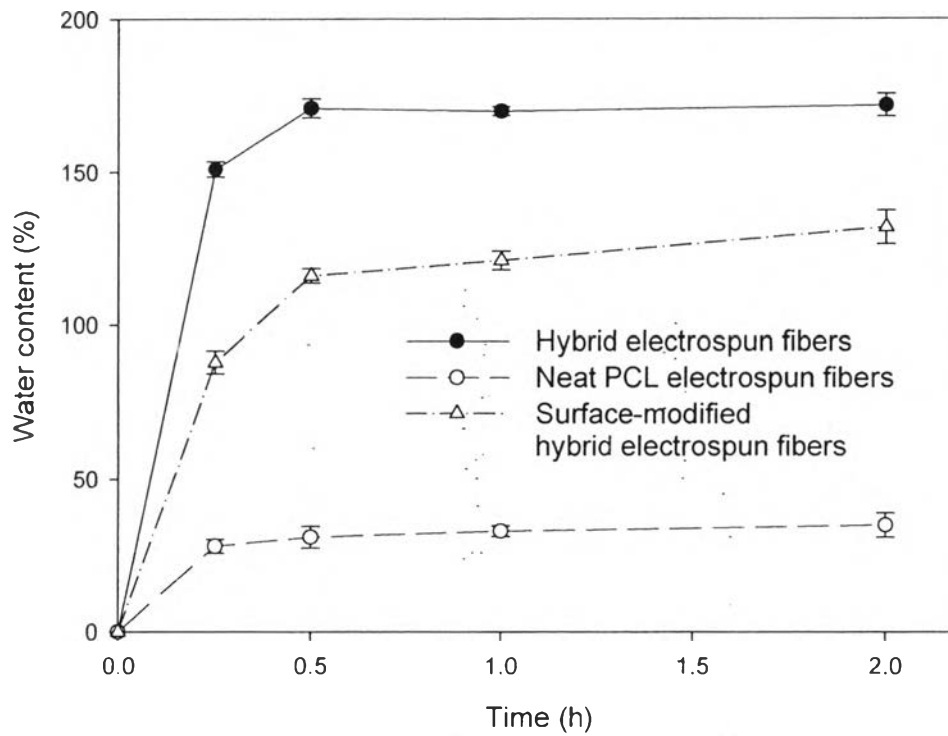
Figure 5.6 Water retention capacity behavior of PCL electrospun fibers (○), hybrid electrospun fibers (●) and surface-modified hybrid electrospun fibers (Δ) in PBS buffer at 37°C.
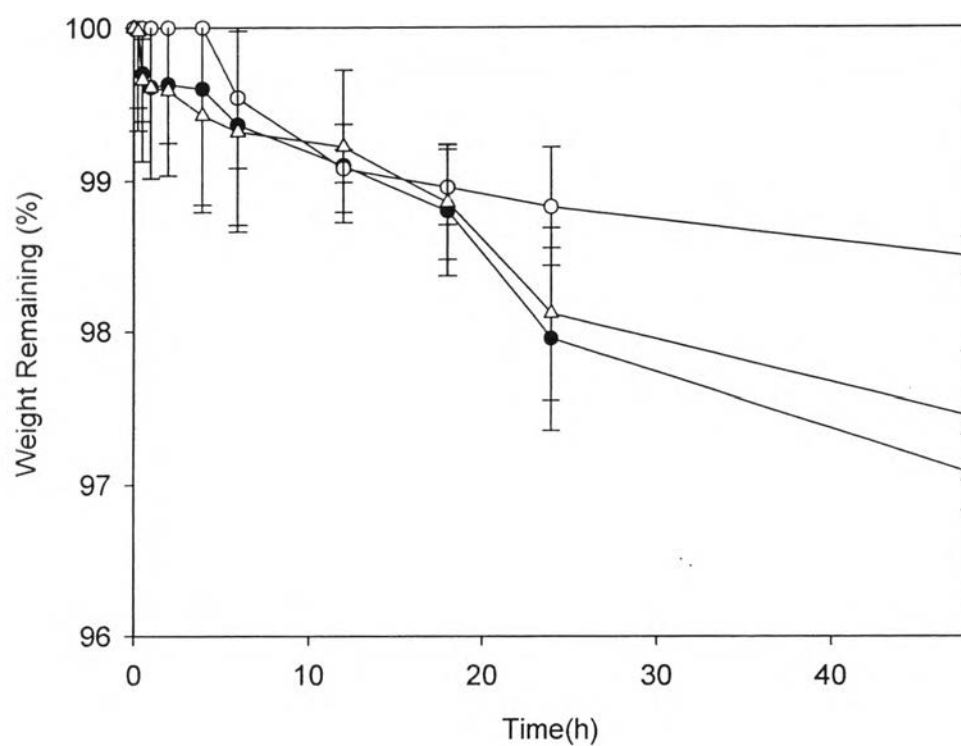
Figure 5.7 Degradation of PCL electrospun fibers (○), hybrid electrospun fibers (●) and surface-modified hybrid electrospun fibers (Δ) as a function of incubation time in PBS buffer at 37°C.
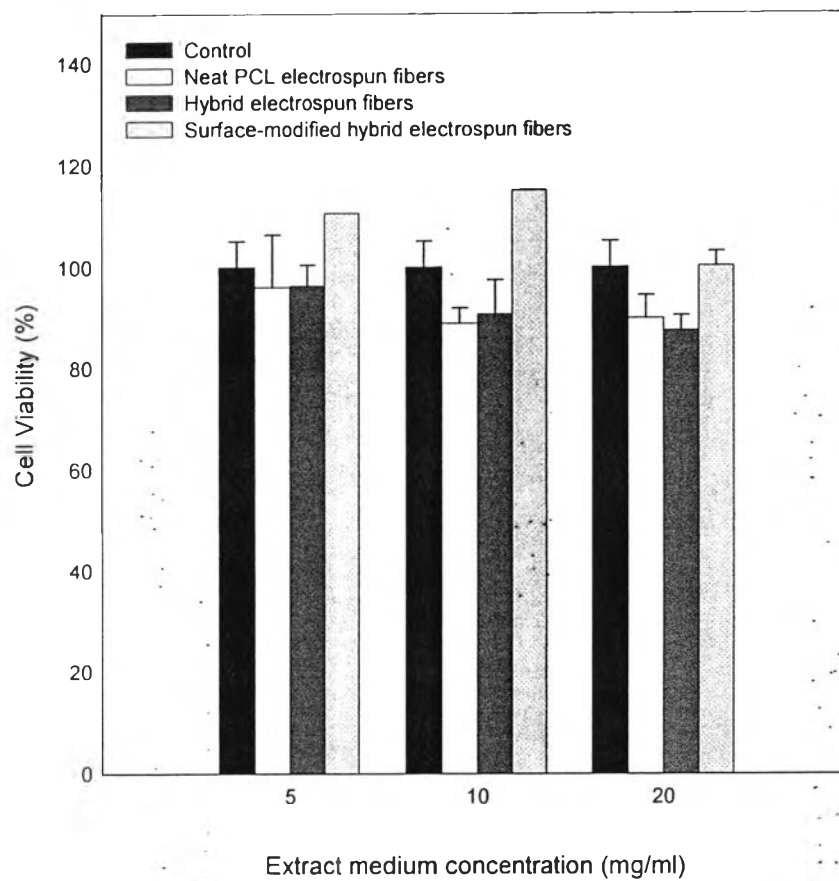
Figure 5.8 Indirect cytotoxicity evaluations for different types of electrospun fibers based on the viability of normal human dermal fibroblasts (NHDF).
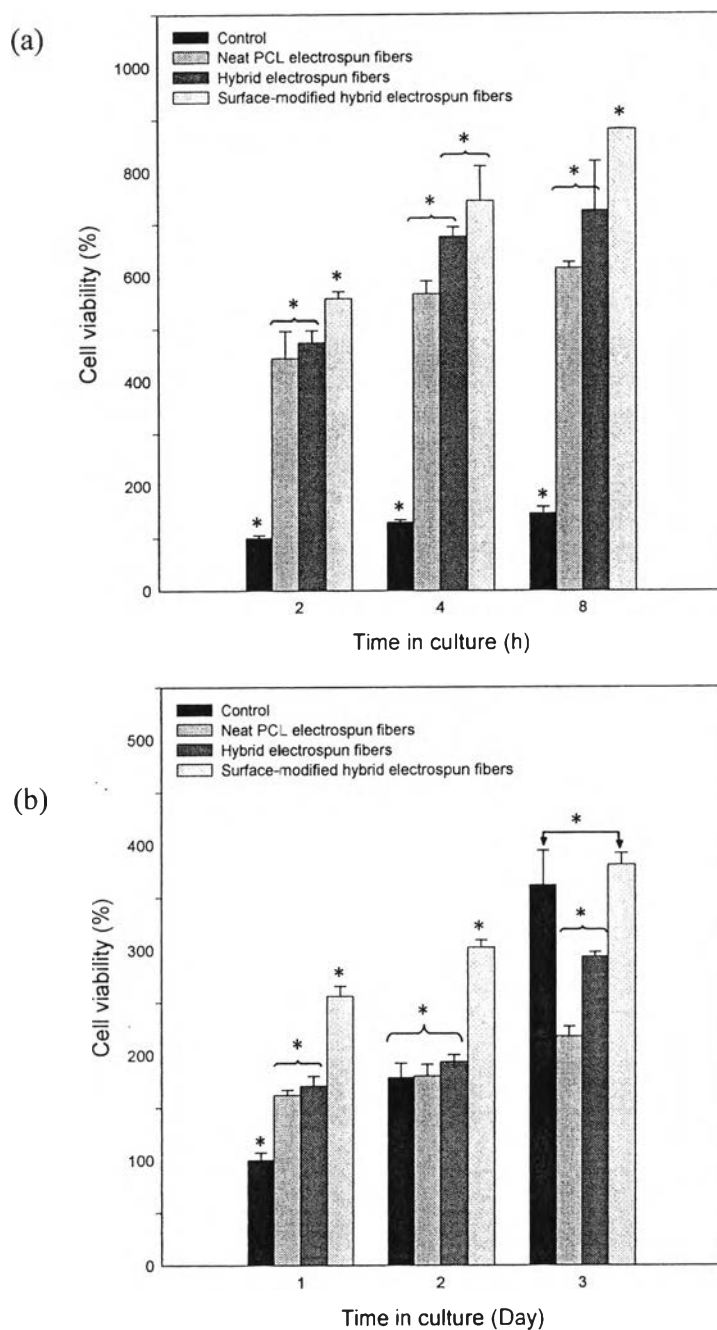
Figure 5.9 Attachment (a) and proliferation (b) of NHDF seeded or cultured on control, PCL electrospun fibers, hybrid electrospun fibers and surface-modified hybrid electrospun fibers as a function of culture time. * Indicates significant difference at p-values of < 0.05

Table 5.3 Representative SEM images of human dermal fibroblast attachment on different types of electrospun fibers after 2h, 4 h and 8 h (magnification = 1000x)
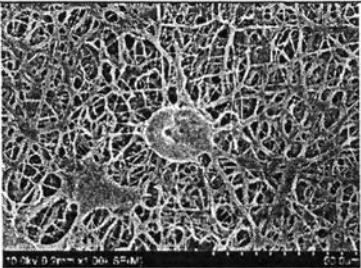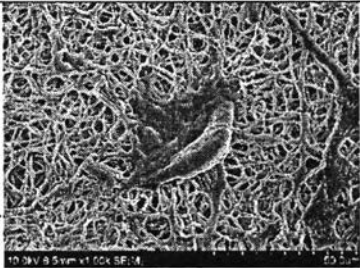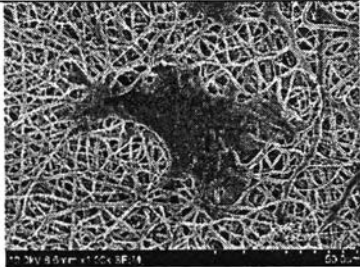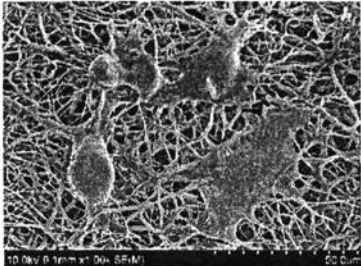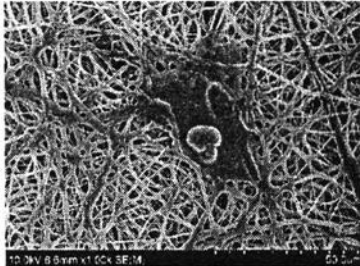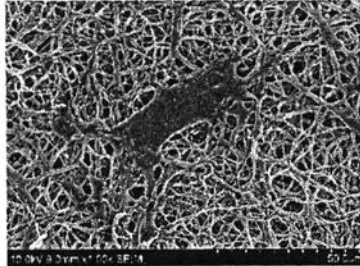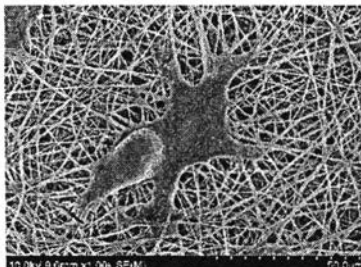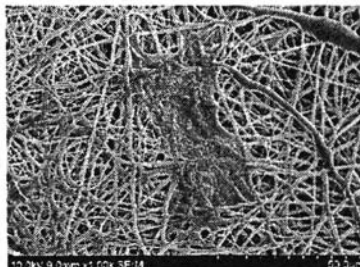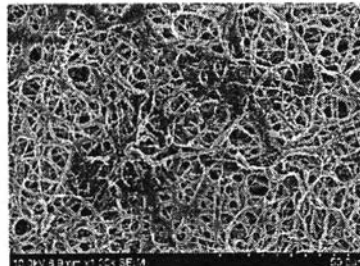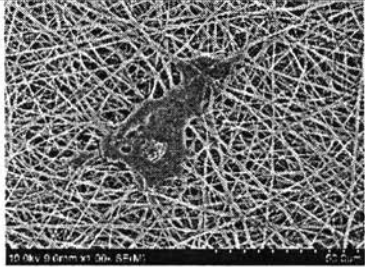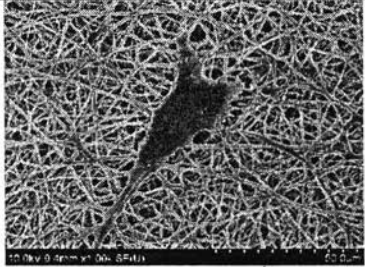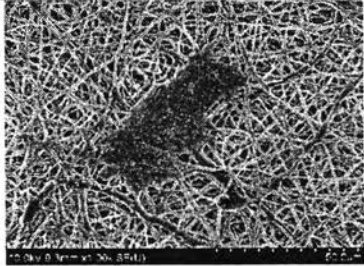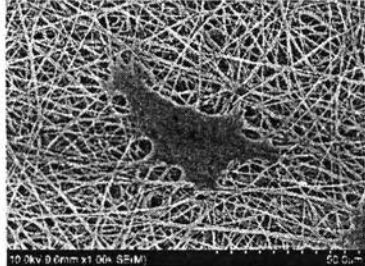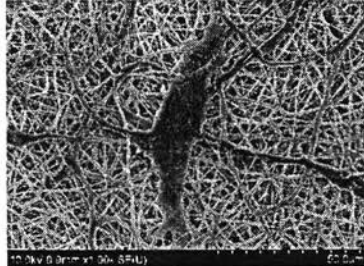
culturing time point	Type of substrate		
	PCL electrospun fibers	Hybrid electrospun fibers	Surface-modified hybrid electrospun fibers
2 hours			
4 hours			
8 hours			

Table 5.4 Representative SEM images of human dermal fibroblast proliferation on different types of electrospun fibers after 1 d, 2 d and 3 d (magnification = 400x, 1000x)

culturing time point	Type of substrate		
	PCL electrospun fibers	Hybrid electrospun fibers	Surface-modified hybrid electrospun fibers
1 day			
2 days			
3 days			